

Mixing and CP violation in the B_d and B_s systems at ATLAS

A. E. Barton

Physics Department, Lancaster University, LANCASTER, LA1 4YB

E-mail: abarton@cern.ch

Abstract. This note includes a measurement of the B_s^0 decay parameters in the $B_s \rightarrow J/\psi\phi$ channel and a measurement of the B^0 meson proper decay time and decay with using the statistics collected by the ATLAS experiment in Run I of the LHC. The first result presents the measurement of the CP -violating phase ϕ_s , the decay width Γ_s and the width difference between the mass eigenstates $\Delta\Gamma_s$. The second result presents the measurement of the width difference $\Delta\Gamma_d$, which is extracted from the measurement of the lifetime dependence of $B^0 \rightarrow J/\psi K_S$ and $B^0 \rightarrow J/\psi K^{*0}$ decays. The obtained results are $\phi_s = 0.098 \pm 0.084(\text{stat.}) \pm 0.040(\text{syst.})$ rad. and $\Delta\Gamma_d/\Gamma_d = (-0.06 \pm 1.42) \times 10^{-2}$.

1. Introduction

ATLAS [1] is a general purpose detector that measures heavy flavour properties using its inner detectors, muon spectrometers and electromagnetic calorimeters (for tagging). Measuring the properties of heavy-flavour particles has been part of the B physics program of the ATLAS experiment since the start of the proton-proton collisions at LHC in 2010. This note presents an overview of recent results obtained using data collected at $\sqrt{s} = 7$ TeV during 2011 and $\sqrt{s} = 8$ TeV during 2012. The analysis of CP violation and mixing can still access physics beyond the standard model; precise measurements may constrain new physics scenarios such as supersymmetry or advance b and c hadron spectroscopy and test QCD.

2. The B_q^0 system

The time evolution of the neutral $B_q^0 - \bar{B}_q^0$ system is described by:

$$\begin{aligned} i \frac{d}{dt} \begin{pmatrix} B_q^0(t) \\ \bar{B}_q^0(t) \end{pmatrix} &= \mathbf{M}_q \begin{pmatrix} B_q^0(t) \\ \bar{B}_q^0(t) \end{pmatrix}, \\ \mathbf{M}_q &= \begin{pmatrix} m_q & m_q^{12} \\ (m_q^{12})^* & m_q \end{pmatrix} - \frac{i}{2} \begin{pmatrix} \Gamma_q & \Gamma_q^{12} \\ (\Gamma_q^{12})^* & \Gamma_q \end{pmatrix}. \end{aligned} \quad (1)$$

The time dependence of the decay rate $B_q^0 \rightarrow f$ is sensitive to f . The time-dependent decay rate is given by:

$$\Gamma(B_q^0(t) \rightarrow f) \propto e^{-\Gamma_q t} \left[\cosh \frac{\Delta\Gamma_q t}{2} + A_{\text{CP}}^{\text{dir}} \cos(\Delta m_q t) + A_{\Delta\Gamma} \sinh \frac{\Delta\Gamma_q t}{2} + A_{\text{CP}}^{\text{mix}} \sin(\Delta m_q t) \right]. \quad (2)$$

Here t is the proper decay time of the B_q^0 meson.

The parameters $A_{\text{CP}}^{\text{dir}}$, $A_{\Delta\Gamma}$ and $A_{\text{CP}}^{\text{mix}}$ depend on the final state f . The abbreviations “dir” and “mix” stand for “direct” and “mixing”. By definition:

$$|A_{\text{CP}}^{\text{dir}}|^2 + |A_{\Delta\Gamma}|^2 + |A_{\text{CP}}^{\text{mix}}|^2 \equiv 1. \quad (3)$$

Assuming that the CP-violating phase ϕ_q^{12} is small, which is experimentally confirmed for both the B^0 and B_s mesons [2]:

$$\Gamma(\bar{B}_q^0(t) \rightarrow f) \propto e^{-\Gamma_q t} \left[\cosh \frac{\Delta\Gamma_q t}{2} - A_{\text{CP}}^{\text{dir}} \cos(\Delta m_q t) + A_{\Delta\Gamma} \sinh \frac{\Delta\Gamma_q t}{2} - A_{\text{CP}}^{\text{mix}} \sin(\Delta m_q t) \right]. \quad (4)$$

The parameters $A_{\text{CP}}^{\text{dir}}$, $A_{\Delta\Gamma}$ and $A_{\text{CP}}^{\text{mix}}$ are theoretically well defined for flavour-specific final states and CP eigenstates [3]. For a flavour-specific final state f_{fs} , such that only the decay $B_q^0 \rightarrow f_{\text{fs}}$ is allowed while $\bar{A}_f = \langle f_{\text{fs}} | \bar{B}_q^0 \rangle = 0$, the parameters are:

$$A_{\text{CP}}^{\text{dir}} = 1, \quad A_{\Delta\Gamma} = 0, \quad A_{\text{CP}}^{\text{mix}} = 0. \quad (5)$$

For a flavour-specific final state \bar{f}_{fs} , such that $A_f = \langle \bar{f}_{\text{fs}} | B_q^0 \rangle = 0$, i.e. only the decay $\bar{B}_q^0 \rightarrow \bar{f}_{\text{fs}}$ is allowed, the parameters are:

$$A_{\text{CP}}^{\text{dir}} = -1, \quad A_{\Delta\Gamma} = 0, \quad A_{\text{CP}}^{\text{mix}} = 0. \quad (6)$$

For the B^0 decay to the CP eigenstate $J/\psi K_s$ the parameters are:

$$A_{\text{CP}}^{\text{dir}} = 0, \quad A_{\Delta\Gamma} = \cos(2\beta), \quad A_{\text{CP}}^{\text{mix}} = -\sin(2\beta), \quad (7)$$

$$\beta = \arg \left(-\frac{V_{cd} V_{cb}^*}{V_{td} V_{tb}^*} \right). \quad (8)$$

If the initial flavour of the B_q^0 meson is not tagged and the mixture of the states is equal and unbiased, the decay rates given by Eqs. (2) and (4) are added together. In this case, the production asymmetry A_{P} of the B_q^0 meson in pp collisions should be taken into account. This asymmetry is defined as:

$$A_{\text{P}} = \frac{\sigma(B_q^0) - \sigma(\bar{B}_q^0)}{\sigma(B_q^0) + \sigma(\bar{B}_q^0)}. \quad (9)$$

The oscillation rates Δm_d and Δm_s have not been measured at ATLAS so the world averages [4] are used in our analyses.

$$\Delta m_d = 0.510 \pm 0.003 \times 10^{12} \text{s}^{-1} \quad (10)$$

$$\Delta m_s = 17.757 \pm 0.021 \times 10^{12} \text{s}^{-1} \quad (11)$$

3. CP Violation

ATLAS has performed a measurement of the CP-violating phase ϕ_s using the 2012 proton-proton dataset [5]. This is done using the exclusive decay $B_s \rightarrow J/\psi(\mu^+\mu^-)\phi(K^+K^-)$, which is a mixture of CP-even and CP-odd eigenstates. CP violation arises from interference between the direct decay and the mixing. From existing measurements, the standard model constrains this to be $\phi_s = -0.04$ rad.

Tagger	Efficiency [%]	Dilution [%]	Tagging Power [%]
Combined μ	4.12 ± 0.02	47.4 ± 0.2	0.92 ± 0.02
Electron	1.19 ± 0.01	49.2 ± 0.3	0.29 ± 0.01
Segment-tagged μ	1.20 ± 0.01	28.6 ± 0.2	0.10 ± 0.01
Jet-charge	13.15 ± 0.03	11.85 ± 0.03	0.19 ± 0.01
Total	19.66 ± 0.04	27.56 ± 0.06	1.49 ± 0.02

Table 1. Summary of tagging performance for the different flavour tagging methods described in the text. Uncertainties shown are statistical only. The efficiency and tagging power are each determined by summing over the individual bins of the charge distribution. The effective dilution is obtained from the measured efficiency and tagging power. For the efficiency, dilution and tagging power, the corresponding uncertainty is determined by combining the appropriate uncertainties in the individual bins of each charge distribution. [5]

The analysis measures the mass, lifetime, three transversity angles and tagging information. These are placed in an unbinned maximum likelihood fit function:

$$\ln \mathcal{L} = \sum_{i=1}^N \{w_i \cdot \ln(f_s(\mathcal{F}_s + f_{B_d^0} \cdot \mathcal{F}_{B_d^0}) + (1 - f_s \cdot (1 + f_{B_d^0}))\mathcal{F}_{\text{bkg}})\} \quad (12)$$

w_i is a per-candidate weight for trigger lifetime efficiency.

The fitted PDF has four components:

$$\mathcal{F}_s = \text{Mass} \cdot \text{Lifetime} + \text{Angles} + \text{Tagging} \cdot \text{Acceptance}$$

$$\mathcal{F}_{B_d^0} = \text{Mass} \cdot \text{Lifetime} \cdot \text{Angles}$$

$$\mathcal{F}_{\text{bkg}} = \text{Mass} \cdot \text{Lifetime} \cdot \text{Angles}$$

The probability density function contains a number of symmetries. As the sign of the $\Delta\Gamma_S$ is not resolved by the data, it is assumed to be > 0 and a measurement from LHCb confirms this [6]. A second ambiguity exists in ϕ_S and the strong phases, this can be resolved by the flavour tagging information.

3.1. Tagging

The analysis uses opposite-side tagging which was calibrated from the B^\pm self-tagging channels. A combination of four tagging methods are used and they can be seen along with their efficiency ϵ , dilution $D = (1 - \omega)$ and power $P = \epsilon D^2$ in the table 1.

3.2. Results

The results from the 2012 data set demonstrate compatibility with the standard model and the 2011 dataset previously published [7]. The combined parameters are calculated using the Best Linear-Unbiased Estimate (BLUE) taking in to account parameter correlations. The results can be seen in table 2, with figures 1 and 2 showing the likelihood contours for the result. Comparisons with other experiments can be seen in figure 3.

3.3. Future performance of detector

ATLAS has released a note which gives estimates of the detector performance after the planned upgrades in the coming years [8]. This includes the IBL (insertable-B-layer) that has been

Par	8 TeV data			7 TeV data			Run1 combined		
	Value	Stat	Syst	Value	Stat	Syst	Value	Stat	Syst
ϕ_s [rad]	-0.109	0.082	0.042	0.12	0.25	0.05	-0.089	0.078	0.041
$\Delta\Gamma_s$ [ps ⁻¹]	0.101	0.013	0.007	0.053	0.021	0.010	0.086	0.011	0.007
Γ_s [ps ⁻¹]	0.676	0.004	0.004	0.677	0.007	0.004	0.675	0.003	0.003
$ A_{\parallel}(0) ^2$	0.229	0.005	0.006	0.220	0.008	0.009	0.227	0.004	0.006
$ A_0(0) ^2$	0.521	0.004	0.007	0.529	0.006	0.012	0.520	0.003	0.007
$ A_S ^2$	0.098	0.008	0.022	0.024	0.014	0.028	0.073	0.007	0.018
δ_{\perp} [rad]	4.50	0.45	0.30	3.89	0.47	0.11	4.16	0.32	0.16
δ_{\parallel} [rad]	3.15	0.10	0.05	[3.04, 3.23]		0.09	3.15	0.10	0.05
$\delta_{\perp} - \delta_S$ [rad]	-0.08	0.03	0.01	[3.02, 3.25]		0.04	-0.08	0.03	0.01

Table 2. Current measurements using data from 8 TeV pp collisions, the previous measurement using data taken at centre of mass energy of 7 TeV and the values for the parameters of the two measurements, statistically combined. [5]

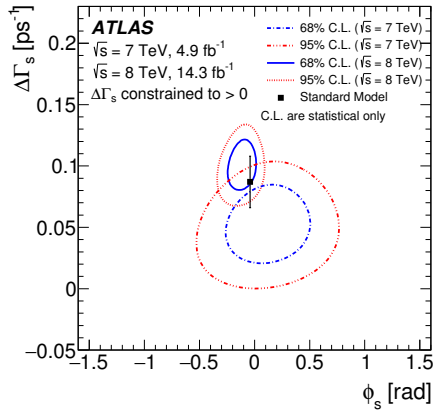


Figure 1. Likelihood contours for the 2011 and 2012 datasets. [5]

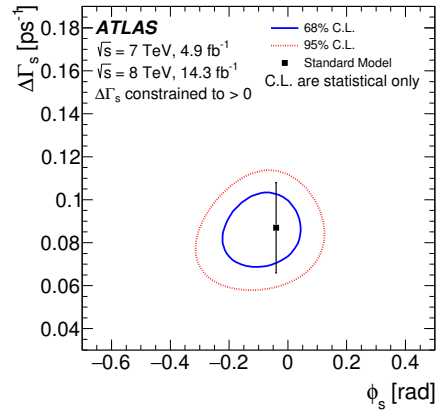


Figure 2. Likelihood contour for the combined result [5]

installed for 2015 and the planned ITK detector that will be installed alongside the High-Luminosity LHC upgrade. Figure 4 shows the proper decay time uncertainty vs the p_T of the decaying B_s meson for the tested detector layouts. Table 3 includes information on the estimated signal yields and the estimated precision of the ϕ_s measurements.

4. Measurement of the relative width difference of the $B_0-\bar{B}_0$ system with the ATLAS detector

$\Delta\Gamma_d$ is one of the least measured parameters in the B mass system. The standard model makes a precise prediction of a small value for $\Delta\Gamma_d^{\text{SM}} = 0.1 \pm 1.0 \times 10^{-2}$. The eigenstate information outlined in section 2 indicates we can measure this using a ratio of events from the decays $B_d^0 \rightarrow J/\psi K^*$ and $B_d^0 \rightarrow J/\psi K_s^0$. This is measured with the 2011 and 2012 datasets recorded by the ATLAS experiment [9].

A_p is the particle/anti-particle production asymmetry. The observed asymmetry A_{obs} is calculated in bins of proper decay length, the asymmetry A_P is then obtained from a χ^2

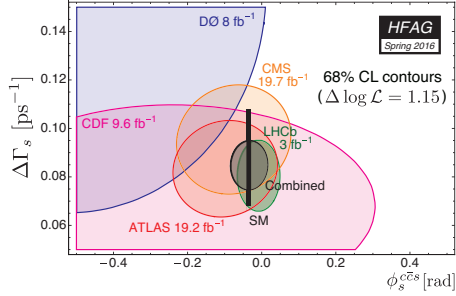


Figure 3. Likelihood contours comparing results from different experiments. [2]

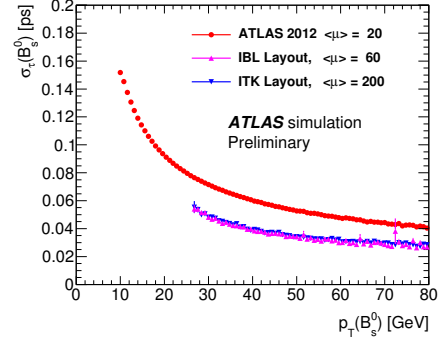


Figure 4. A plot showing the proper decay time uncertainty vs the p_T of the decaying B_s meson of the current and future ATLAS detectors. [8]

	2011	2012	2015-17		2019-21	2023-30+
Detector	current	current	IBL		IBL	ITK
Average interaction per BX $\langle \mu \rangle$	6-12	21	60		60	200
Luminosity, fb^{-1}	4.9	20	100		250	3 000
Di- μ trigger p_T thresholds, GeV	4-4(6)	4-6	6-6	11-11	11-11	11-11
Signal events per fb^{-1}	4 400	4 320	3 280	460	460	330
Signal events	22 000	86 400	327 900	45 500	114 000	810 000
Total events in analysis	130 000	550 000	1 874 000	284 000	758 000	6 461 000
MC $\sigma(\phi_s)$ (stat.), rad	0.25	0.10	0.045	0.083	0.053	0.018

Table 3. Estimated ATLAS statistical precisions ϕ_s for considered LHC periods. Values for 2011 and 2012 in this table are derived using the same method as for future periods. [8]

minimisation where A_{det} is the detector reconstruction asymmetry:

$$A_{i,obs} \equiv \frac{N_i(J/\psi K^{*0}) - N_i(J/\psi \bar{K}^{*0})}{N_i(J/\psi K^{*0}) + N_i(J/\psi \bar{K}^{*0})}, \quad (13)$$

$$\chi^2[A_{det}, A_p] = \sum_{i=2}^{10} \frac{(A_{i,obs} - A_{i,exp})^2}{\sigma_i^2}. \quad (14)$$

The detector asymmetry A_{det} and A_p are fit to obtain values of $A_{det} = (+1.33 \pm 0.24 \pm 0.22) \times 10^{-2}$ and $A_p = (+0.25 \pm 0.48 \pm 0.05) \times 10^{-2}$. The A_p is found to be consistent with LHCb, although since ATLAS is observing a different region it does not need to be equivalent.

The mass spectrum are fitted in each proper decay length bin to extract the yields. Examples of the fits can be seen in figures 5 and 6. Each bin has an efficiency correction ratio applied, this ratio is determined using Monte Carlo data.

The final results are $\Delta\Gamma_d/\Gamma_d = (-2.8 \pm 2.2(\text{stat.}) \pm 1.5(\text{MC stat.})) \times 10^{-2}$ for the 2011 dataset and $\Delta\Gamma_d/\Gamma_d = (+0.8 \pm 1.3(\text{stat.}) \pm 0.5(\text{MC stat.})) \times 10^{-2}$ for the 2012 dataset. These results are combined using the χ^2 method. Correlations between sources of systematics common to the two datasets are taken into account. The systematic uncertainty due to the

background description and the MC are considered to be uncorrelated. This combined result is $\Delta\Gamma_d/\Gamma_d = (-0.1 \pm 1.4) \times 10^{-2}$. This combined result is currently the most precise single measurement of this quantity, it agrees with the standard model prediction and the indirect measurement by D0.

The fact the asymmetry is a ratio cancels out most biases from the trigger, time resolution or B production properties. However, differences between the channels and simulation inaccuracies could remain. The systematics uncertainties are thus estimated and shown in table 4.

Source	$\delta(\Delta\Gamma_d/\Gamma_d)$, 2011	$\delta(\Delta\Gamma_d/\Gamma_d)$, 2012
K_S decay length	0.21×10^{-2}	0.16×10^{-2}
K_S pseudorapidity	0.14×10^{-2}	0.01×10^{-2}
$B^0 \rightarrow J/\psi K_S$ mass range	0.47×10^{-2}	0.59×10^{-2}
$B^0 \rightarrow J/\psi K^{*0}$ mass range	0.30×10^{-2}	0.15×10^{-2}
Background description	0.16×10^{-2}	0.09×10^{-2}
$B_s \rightarrow J/\psi K_S$ contribution	0.11×10^{-2}	0.08×10^{-2}
L_{prop}^B resolution	0.29×10^{-2}	0.29×10^{-2}
Fit bias (Toy MC)	0.07×10^{-2}	0.07×10^{-2}
B^0 production asymmetry	0.01×10^{-2}	0.01×10^{-2}
MC sample	1.54×10^{-2}	0.45×10^{-2}
Total uncertainty	1.69×10^{-2}	0.84×10^{-2}

Table 4. Sources of systematic uncertainty in the $\Delta\Gamma_d/\Gamma_d$ measurement and their values for the 2011 and 2012 data sets. [9]

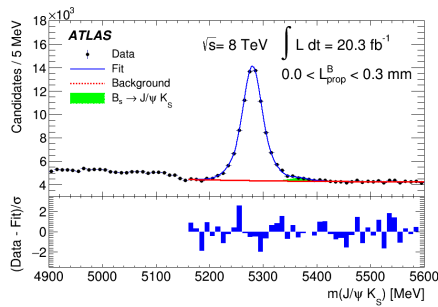


Figure 5. The $J/\psi K_S$ mass fit [9]

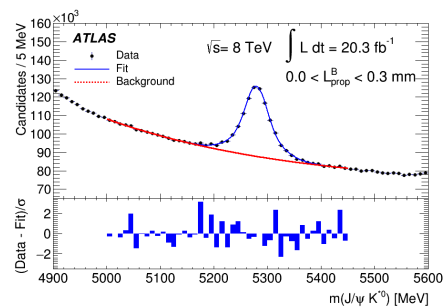


Figure 6. The $J/\psi K^{*0}$ mass fit [9]

References

- [1] ATLAS Collaboration, *J. Instrum.* *3* (2008) S08003.
- [2] Y. Amhis *et al.* (Heavy Flavour Averaging Group), arXiv:1412.7515 [hep-ex].
- [3] A. S. Dighe *et al.* *Eur. Phys. J. C* *6* 647 1999.
- [4] K.A. Olive *et al.* (Particle Data Group), *Chin. Phys. C*, *38*, 090001 (2014).
- [5] ATLAS Collaboration, arXiv:1601.03297 [hep-ex].
- [6] LHCb Collaboration, R. Aaij *et al.* *Phys.Rev.Lett.* *108* (2012) 241801
- [7] ATLAS Collaboration, *Phys.Rev.* D90 (2014) 052007, arXiv:1407.1796 [hep-ex].
- [8] ATLAS Collaboration, ATL-PHYS-PUB-2013-010.
- [9] ATLAS Collaboration, *JHEP06* (2016) 081, arXiv:1605.07485 [hep-ex].